atmosphere

MDPI

Article

Analysis and Mapping of Sea Breeze Event Time in Coastal Cities: A Case Study of Sendai

Shiyi Peng * and Hironori Watanabe

Department of Architecture, Faculty of Engineering, Tohoku Institute of Technology, 35-1 Yagiyamakasumicho, Taihaku Word, Sendai 982-8577, Japan
* Correspondence: d203901@st.tohtech.ac.jp

Abstract: Due to global warming and urbanization, high-temperature events—which frequently occur in cities—are presenting an increasing threat to the daily lives of human beings. In coastal cities, sea breezes can cool the near surface and improve the urban environment to some extent. Understanding the cooling characteristics of sea breeze on the urban environment is informative for improving and mitigating the urban heat island (UHI) effect. In this paper, we analyze the basic characteristics of the timing of the cooling effect of sea breeze in urban summer based on the long-term multi-point measurements of air temperatures. Additionally, the Weather Research and Forecasting (WRF) model is used to show the influence of sea breeze on cities in terms of the cooling action time. The whole process is reproduced based on a time distribution map created using the results of the WRF simulation. The measured temperature and WRF simulation results are also evaluated with observations. The results show little difference between the two. The analysis of the distribution map shows that the sea breeze gradually penetrates inland from coastal areas. It can therefore be concluded that the sea breeze blows at different speeds in different areas. Our results show that the sea breeze is weak in places near the coast, while it is significantly stronger around inland rivers. Moreover, in urban areas that are far from inland rivers, the speed of the sea breeze is evenly distributed in space. The spatial pattern of sea breeze retreat time and arrival time is reversed: retreats happen earlier in inland areas. The duration of the sea breeze shows a significantly decreasing trend from the coast to inland, with the longest duration at the southern end of the urban area near the coast.

Keywords: coastal cities; global warming; sea breeze cooling action; time distribution map; weather research and forecasting (WRF)

Citation: Peng, S.; Watanabe, H. Analysis and Mapping of Sea Breeze Event Time in Coastal Cities: A Case Study of Sendai. *Atmosphere* **2022**, *13*, 1484. https://doi.org/10.3390/atmos13091484

Academic Editors: Sen Chiao, Robert Pasken, Ricardo Sakai and Belay Demoz

Received: 8 August 2022
Accepted: 10 September 2022
Published: 13 September 2022

1. Introduction

Sea breeze is a mesoscale atmospheric phenomenon. In the morning, as the sun rises, the land gradually warms up after absorbing the sun's radiation, while the temperature of the ocean changes very little. This difference in thermal characteristics creates a contrast in air temperature between land and ocean. The resulting pressure gradient from the ocean to the land drives cold shallow ocean air inland, resulting in a sea breeze [1,2].The greater temperature difference between land and sea in summer makes the sea breeze always prevail in coastal cities [3].

As cold ocean air moves landward, the air is gradually heated, and the effect of the sea breeze gradually diminishes to disappear with it, usually affecting land for about a few dozen kilometers [4]. Although the impact is limited in scope, sea breezes have been found to interact significantly with the internal climate of the urban environment [5,6]. Especially when the urban heat island effect is enhanced, the temperature difference between the sea and the land increases, and the sea breeze effect is significantly enhanced [7].

While the sea breeze cools down the temperature, it also brings pollution transport and heat wave diffusion to the coastal areas of many cities [4–8]. Over the past few decades,

global heat wave events have increased each year, with most cities suffering stronger heat wave intensities that last longer [9]. The rise in heat wave events has been attributed to global warming [10] and urban sprawl resulting in high-density urban form with low-density vegetation cover and increasing artificial heat removal [11]. The urban heat island phenomenon not only threatens human health and comfort [12], but also increases the consumption of water and electricity resources [13].

Human overexploitation of the Earth has changed the ground surface conditions and has caused significant changes in the urban climate of coastal areas. Fortunately, it has been found that when wind speed reaches a certain threshold, it can effectively mitigate the urban heat island phenomenon even to the point of complete offset [14]. In particular, this refers to the cold wind from the sea and rivers [3,15]. Sea breezes are therefore seen as an efficient source of cooling that can mitigate urban heat islands [2,16]. The effect of wind on the control of urban temperature has been verified by long-term measurements [17], and it was found that the sea breeze entering the city reduces the urban temperature by about 4 °C compared to the case without wind [18]. This not only improves human comfort, but also effectively reduces energy consumption [19–21] and generates wind energy [22]. Therefore, studies related to sea breeze are very important.

Usually, we divide the factors affecting sea breeze events into natural and human factors. The natural factors include atmospheric conditions, coastal morphology, inland rivers, and forested green spaces. The human factor mainly refers to the ground surface conditions and urban form that have been artificially modified. The current transformation of pristine land is no longer adequate for human activities, and changes in the coastline due to land reclamation are clearly visible on satellite images. The shape of the coastline affects the strength of the sea breeze as it enters the land, and it has been found that the sea breeze is stronger in the cape region and weaker in the bay region [23]. Furthermore, the effects of sea breeze can be enhanced if the location of urban cities is away from the coastline. This is because the cities along the coastline would reduce the strength of sea breeze [24,25]. Such a reinforcing effect also occurs near inland rivers, which have been found to enhance the penetration of sea breezes inland [26], and complex topography has a strong influence on sea breezes [27], while the cooling effect of sea breezes often depends on cold air in areas such as seashores, riversides, and forested green spaces [2]. The artificially modified surface conditions alter the surface energy balance and have a significant impact on ground surface conditions [28,29]. The effect of urban structure on the circulation of sea breeze in coastal cities has been studied extensively [30,31], and it has been found that the roughness of the urban surface has a large effect on the intensity of sea breeze [32], which significantly weakens the intensity of sea breeze [5,6] and leads to a decrease in wind speed in urban areas [33].

Sea breezes have always been studied by means of observational data as well as numerical simulations. There are many ways to obtain data and analyze them. In the early days, sea breezes were analyzed from pure theory. Then, aircraft tracking [34] and LIDAR data inverse analysis [35] were used. In Japan, it has been concluded from the analysis of long-term multi-point test data that sea breezes in coastal areas mitigate temperature rises earlier than the inland areas of Sendai [36]. The cooling effect of sea breeze on the built environment was found to be significant after field measurements in the Fukuoka area, and the sea breeze temperature increased, moving progressively deeper inland [37]. There are also many studies on the acquisition of data by means of numerical simulations. Simulations using mesoscale meteorological studies and forecasting WRF models have revealed that the urban heat island effect increases the temperature difference between the ocean and the land, thus enhancing the sea breeze effect [7]. The cooling effect of sea breeze has been estimated from the wind speed values simulated by the WRF model [38]. Urban environmental climate maps were also produced using the WRF calculations, reproducing the range of sea breeze cooling effects and the range of specific humidity rise effects [39].

In terms of the timing of sea breeze event, it has been found that, if the urban heat island effect is intensified in the morning, then this can lead to an earlier onset of sea

breeze [40]. A strong correlation was also found between the time of arrival and retreat of the sea breeze and the distance and topography of the nearest coastline [41]. However, few studies have discussed the time of action of the sea breeze in an urban context. In this study, temperature data and specific humidity data were obtained by simulating the Sendai region of Japan using the WRF model based on the characteristics of sea breeze event. The study also reproduces the spatial distribution map of the arrival time, retreat time and duration of the sea breeze within the Sendai area. This basic research is finally presented in a clear and concise visualization, which provides a visual understanding of the spatial distribution of sea breeze event times.

2. Data and Methods

2.1. Study Area

Sendai is the capital city of Miyagi Prefecture and is the largest metropolis in northeast Japan, covering an area of 785.8 km^2 (Figure 1b). The southeast is plain, the downtown is hilly, and the northwest is mountainous. The city stretches about 40 km from the southeastern coastline to the northwest. Sendai has a mild subtropical monsoon climate, with hot summers. During the summer days, the wind from the southeast direction from the sea is the most frequent and can effectively reduce the urban temperature of Sendai. Most mountainous coastal cities have urban areas close to the coastline, while the city center of Sendai is about 9 km away from the coastline. Currently, the annual average temperature in Sendai is rising at a rate of 2.3 °C per 100 years, and a detailed analysis of the urban climate is urgently needed.

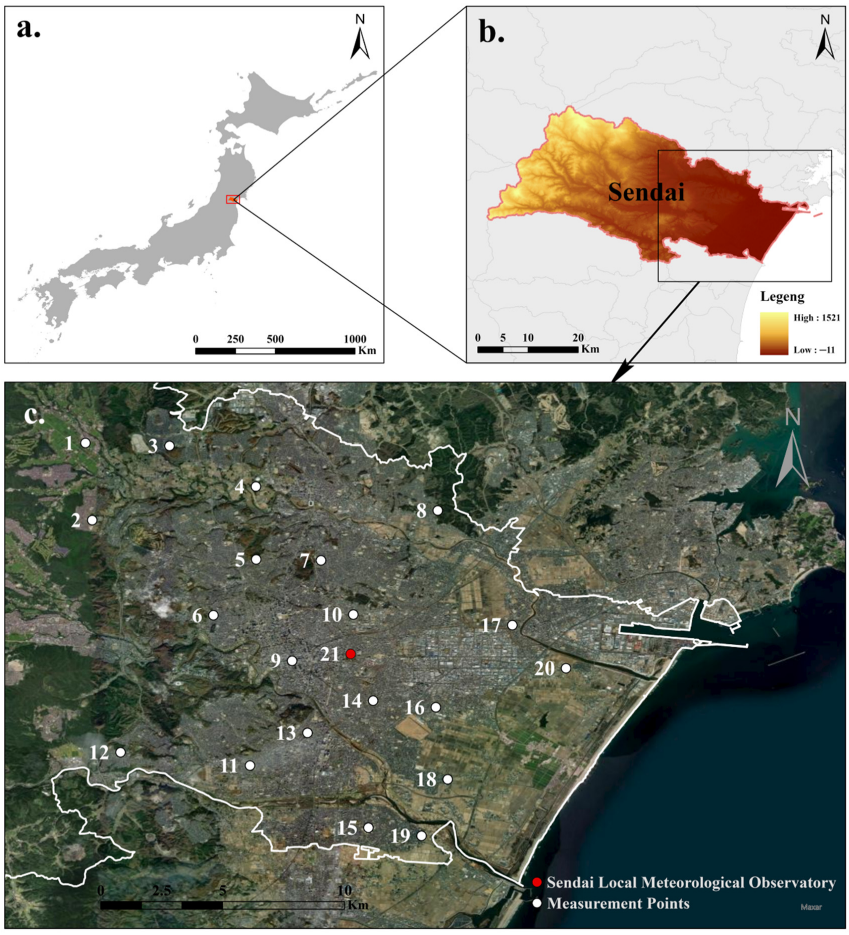

Figure 1. Map showing the location of Sendai and the distribution of temperature and humidity recorders and Sendai Local Meteorological Observatory in the study area. (**a**) Map of Japan; (**b**) topography of Sendai area; (**c**) distribution of temperature and humidity recorders on satellite maps.

2.2. Data

2.2.1. Data Used to Identify Sea Breezes

Sea breeze always appears in warm seasons. We chose only summer as the research object in our study. June, July and August are usually defined as summer. In this study, data from Sendai Local Meteorological Observatory, long-term multi-point measurement data, and data from WRF model calculations were used. We used data from the meteorological observatory to analyze Sendai's climate and to determine the number of sea breeze days. The data are then collated by long-term multi-point measurement data for all sea breeze days. From the collated data, a day that can reflect most of the sea breeze day state is selected as the target study day; the sea breeze event time and characteristics are analyzed in detail, and finally, the sea breeze event map is drawn by the WRF model calculation data, in which the observed data and the WRF model calculation data are verified in detail.

2.2.2. Measurement Data

The measured data used in this study include meteorological observatory data and long-term multi-point measurement data in the research laboratory. The distance from the coast to Sendai Local Meteorological Observatory (38°15′43.60″ N, 140°53′49.52″ E), an urban area, is about 9 km. The south side of the meteorological observatory is a park, the north and east sides are covered by buildings, and the instruments are placed in the open space on the west side of the weather bureau building. Various meteorological variables were recorded, such as air temperature, humidity, wind direction and velocity, sunlight intensity, precipitation and atmospheric pressure. All data can be obtained from the Japan Meteorological Agency, where the wind speed indicates its instantaneous and average values. The humidity measurement used an electronic hygrometer, and the thermometer was mounted at a height of 1.5 m above the ground. They were recorded at a frequency of 10 min.

Long-term multi-point test data were obtained from 20 temperature and humidity sensors (Table 1). The measuring instrument used a temperature and humidity recorder (T&D Corporation), and the frequency of data recording wase set to 10 min (Figure 2). In order to avoid both rain and direct sunlight and to satisfy the need to record data in a naturally ventilated state, the measuring instruments were installed in instrument shelter. All the instrument shelters were placed in the playgrounds of primary schools or in parks within Sendai city (Figure 1c). To avoid local effects on measurements, the instrument shelters were placed away from trees and building walls. Twenty measurement points extended inland from the city coast. A total of six measurement points were set up within 7 km from the coast, with four points inland after 15 km, and the rest of the points were distributed in the city.

Figure 2. Installation status of the measuring equipment in the louver and temperature and humidity recorder, RH TR-72U.

Table 1. Temperature and humidity recorder, and Sendai Local Meteorological Observatory information, including ID, name, coordinates and distance from the coast in the direction of prevailing winds.

ID	Location	Lon.	Lat.	Distance (Km)
1	Nenoshiroishi	140.796602	38.341726	21.35
2	Yakata	140.799167	38.312591	19.68
3	Teraoka	140.828391	38.340624	18.92
4	Nomura	140.861097	38.325285	15.65
5	Kita-Sendai	140.861212	38.297756	13.91
6	Kunimi	140.845	38.27666667	14.02
7	Asahigaoka	140.885703	38.297379	12.15
8	Tsurugaoka	140.929878	38.316229	10.15
9	Higashi Nibancho	140.874781	38.259458	10.82
10	Saiwaicho	140.897926	38.276957	10.00
11	Nishitaga	140.858828	38.219923	11.63
12	Hitokita	140.809892	38.224932	14.75
13	Nagamachi	140.880617	38.232263	8.98
14	Minamikoizumi	140.905447	38.244434	7.61
15	Fukurobara	140.903682	38.196458	5.92
16	Kabanomachi	140.9291667	38.24194444	5.60
17	Takasago	140.958098	38.272964	5.27
18	Rokugo	140.9336111	38.21472222	3.75
19	Higashishiromaru	140.923753	38.193381	4.15
20	Okada	140.978404	38.256679	2.83
21	Observatory	140.89692	38.26209	9.43

2.2.3. WRF Model and Experimental Design

In this study, we used the Advanced Research Weather Research and Forecasting (ARW-WRF) model developed by the National Center for Atmospheric Research (NCAR) and the National Center for Environmental Prediction (NCEP) to numerically simulate the Sendai urban area [42,43]. The main physical settings of the model are shown in Table 2. These settings are similar to those used in a [39] study of the extent of sea breeze cooling in the Sendai area. In this simulation, we used three nested domains (Figure 3). The outer square is domain 1, which consists of 37 × 28 grids with a spatial resolution of 9 km. Domain 2 consists of 43 × 34 grids with a spatial resolution of 3 km. The main analysis domain is domain 3, which consists of 31 × 28 grids with a spatial resolution of 1 km. A horizontal resolution of 1 km is widely used in numerical studies of urbanization and sea breeze [34,44,45]. The number of vertical layers used in this study was 30, and the urban canopy model [46] and WSM 6-class graupel scheme [47] were used. There are many planetary boundary layer (PBL) schemes available, and some researchers have made detailed comparisons of the different schemes [48]. For this simulation, we used the Mellor–Yamada–Janjic model [24]. The Rapid Radiative Transfer Model for General circulation models (RRTMG) longwave scheme and Dudhia shortwave scheme in the general circulation model were used. The land data utilized data from the Digital Land Information released by the Japanese government in space with a resolution of 1 km. The initial boundary conditions for the simulations were generated from the final operational global analysis data (FNL) from the National Center for Environmental Prediction (NCEP). The calculation period was from 1 to 10 August 2016. The simulated data in domain 3 finally generate 31 × 28 point data, and each point datum contains the values of temperature at 2 m above ground and specific humidity at 2 m above ground. The frequency of the numerical output is 10 min, which is the same as the measured data.

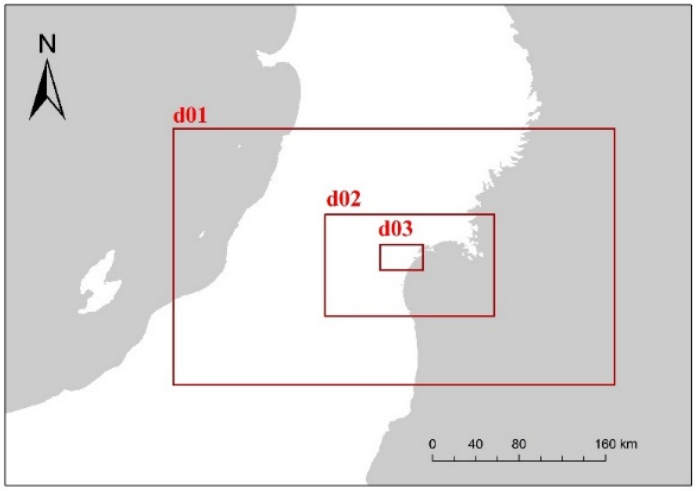

Figure 3. Definition of the three domains for the WRF model.

Table 2. Domains and parameterization schemes used in WRF model experiments.

Calculation period	09:00 (JST) on 1 August 2016, to 09:00 (JST) on 10 August 2016
Vertical grid	30 layers
Horizontal grid (Figure 3)	Domain 1: 9 km, dimension 37 × 28 Domain 2: 3 km, dimension 43 × 34 Domain 3: 1 km, dimension 31 × 28
Meteorological data	NCEP re-analysis of global objective data
Land data	Digital national land information (resolution of 1000 m)
Microphysics	WSM 6-class graupel scheme [47]
Radiation: **Longwave** **Shortwave**	 Rapid radiative transfer model Dudhia shortwave
PBL scheme	Mellor–Yamada–Janjic TKE scheme [24]
Surface scheme	Urban canopy model [46]
Cumulus scheme	Kain–Fritsch scheme [49]

2.3. Identification of Sea Breezes

We identified the sea breeze days by the meteorological observatory data downloaded from the Japan Meteorological Agency. Therefore, we identified sea breeze days by the generation of sea breeze and the characteristics of the meteorological variables that change after the occurrence of sea breeze. Additionally, to exclude the interference of other factors, we selected sunny days for the identification of sea breeze days. Specifically, these included the following:

Sunshine: 40% or more of the possible sunshine hours.
Cloud: less than 5% cloud.
Rainfall: no rainfall.
Wind: wind blowing from the sea to the land lasting at least 2 h.
Temperature: a drop in temperature lasting 1 h or more after the start of the sea breeze.

3. Basic Characteristics of Summer Sea Breeze Activity in Sendai

3.1. Representative Validation of the Study Period

In this study, data from Sendai local meteorological observatory were used to analyze and organize the climate characteristics of Sendai city in summer. The study period was chosen to be three years, 2018–2020. We compared the three-year study period (August 2018

to 2020, Period B) with a twelve-year period (August 2010 to 2021, Period A) for both periods. The summer sea breeze days of the two periods were screened, and then, the daily average temperature curves of the sea breeze days of the two periods were overlapped (Figure 4). The overlap revealed that the two data points overlap well. Therefore, we believed that the study period is a good representation of the temperature characteristics of the sea breeze days in Sendai in summer.

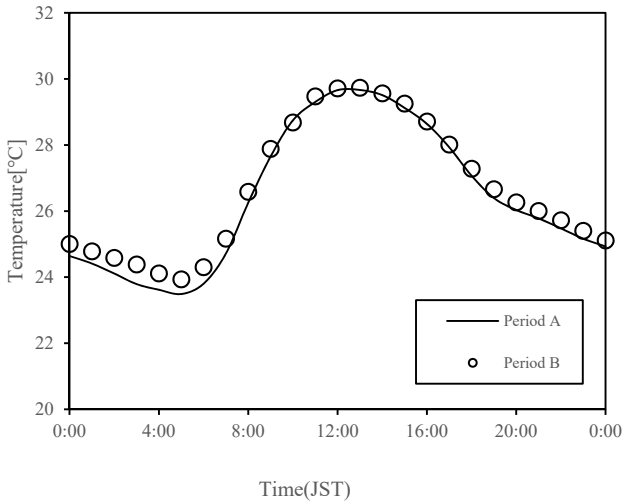

Figure 4. Average diurnal temperature fluctuations at Sendai Local Meteorological Observatory during period A (August 2010 to 2021) and period B (August 2018 to 2020) on sea breeze days.

3.2. Define the Research Month

Sea breezes usually occur in warm seasons, and since the focus of this study is on sea breeze event, the statistics focus on the characteristics of hot summer weather. According to the 3-year monthly mean temperature curves of the study period (Figure 5a), the highest monthly mean temperature in 2019 and 2020 occurred in August, and the highest monthly mean temperature in 2018 occurred in July, followed by August. Of these, the highest-temperature days in 2018 and 2020 occurred in August, and the highest-temperature day in 2019 occurred in July (Figure 5b). Finally, the number of days with maximum temperatures greater than 30 °C in June, July and August for the three years of the study period was counted. Most of the days are concentrated in July and August, with more than half of the days in 2019 and 2020 occurring in August. This shows that hot days are most common in August. Therefore, we have made August our focus month of study (Figure 6).

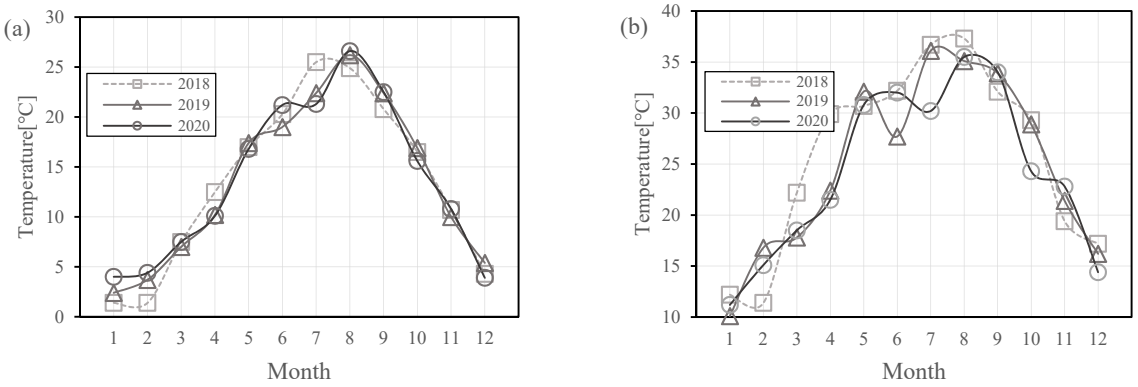

Figure 5. (**a**) Monthly average temperature from 2018 to 2020; (**b**) monthly maximum temperature from 2018 to 2020.

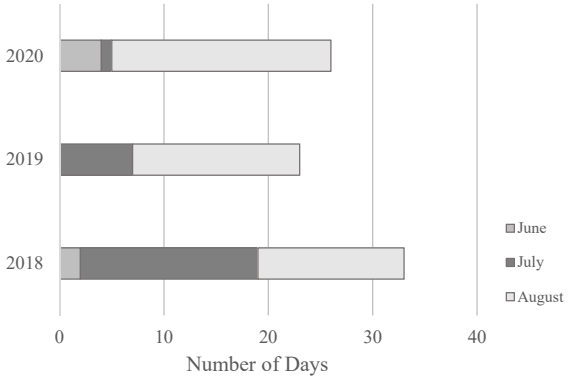

Figure 6. Number of days with daily maximum temperature greater than 30 degrees Celsius in July–August–September from 2018 to 2020.

3.3. August Sea Breeze Daily Temperature Characteristics

We collated the temperatures for all sea breeze days in August during the study period. The number of sea breeze days increased each year from 2018 to 2020. In 2020, more than 20 days were defined as sea breeze days. Additionally, in any given year, more than half of the days identified as sea breeze days had high temperatures greater than 30 °C (Figure 7). From this, we can find that the temperature is usually very high on sea breeze days.

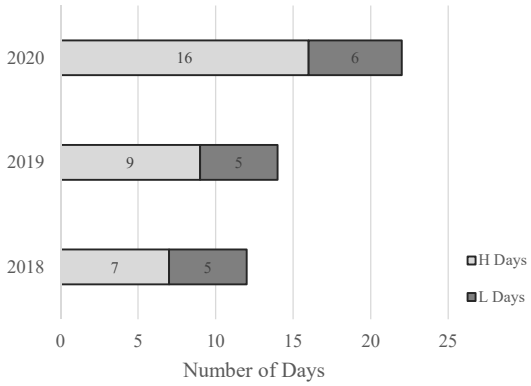

Figure 7. Number of days with maximum temperatures above 30 degrees Celsius (H Days) and below 30 degrees Celsius (L Days) for August 2018 to 2020 and defined as sea breeze days.

4. Temporal Characteristics of Sendai Sea Breeze Event

4.1. Analysis of Sea Breeze Event Time Characteristics

Unlike the previous definition of sea breeze arrival and retreat times by wind conditions, we determined the sea breeze arrival and retreat times based on the variation in sea breeze daily temperature and specific humidity (Figure 8). When the sun rises, the temperature of the land begins to rise, forming a pressure difference with the sea, and the air begins to move from the sea to the land. The wind blowing from the direction of the sea brings cold air to the land; thus, we define the point in time when the temperature starts to drop after sunrise as the time when the sea breeze arrives. The continuous rise in temperature is suppressed when the sea breeze arrives, at which point it lowers the temperature of the city. Additionally, it also brings humidity. The temperature fluctuates in a constant range, and the humidity rises again after a significant drop at midday due to strong sunlight. Because of the weakening of insolation, the temperature starts to exceed the constant range, and the rate of decrease increases significantly. At this point, the specific humidity also drops sharply once again, and we define this moment as the time of retreat of the sea breeze.

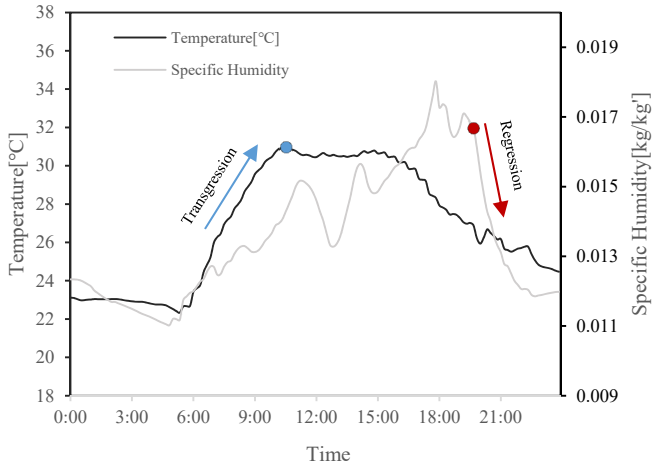

Figure 8. The diurnal temperature fluctuations and diurnal specific humidity fluctuations for 5 August 2016. The points pointed by the arrows show the time of arrival (blue points) and retreat of the sea breeze (red points).

4.2. Sea Breeze Arrival Time Distribution Pattern

The total number of sea breeze days in August during the study period was 48 days. The sea breeze arrival time was distributed between 8:00–16:00, concentrated between 10:00–13:00, and 11:00 was the most common time for most days (Figure 9a).

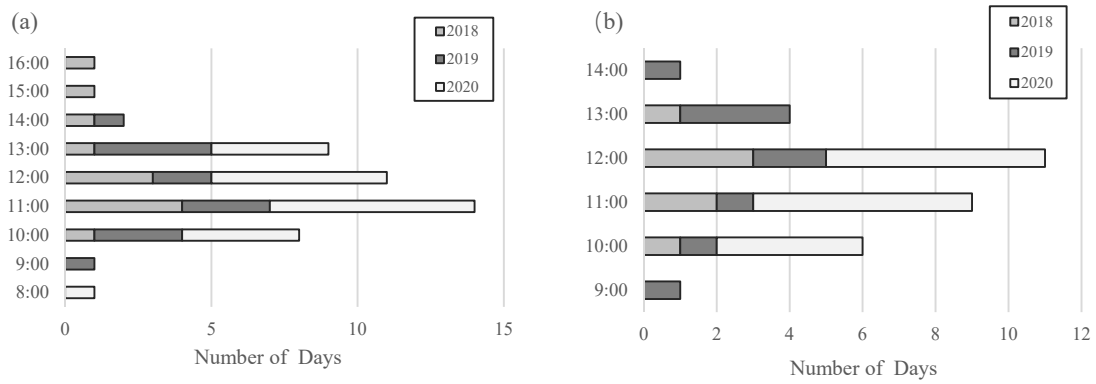

Figure 9. (**a**) Sea breeze arrival times for all sea breeze days in August from 2018 to 2020. (**b**) Sea breeze arrival times for August sea breeze days with maximum temperatures above 30 degrees Celsius from 2018 to 2020.

Of all sea breeze days in August during the study period, the maximum temperature was greater than 30 °C on a total of 32 days. The sea breeze arrival time on these days was distributed between 9:00 and 14:00, concentrated between 10:00 and 12:00, and 12:00 was the most common time for most days (Figure 9b).

Therefore, in determining the case study days, we chose days when the sea breeze occurred at the time of 11:00 or 12:00.

4.3. Case Study Day

According to the above rule, we chose the days when the sea breeze arrived at 11:00 or 12:00. On the basis of meeting the conditions of sea breeze day identification, in order to reduce the disturbing factors, in the daylight requirements, we chose days with all-day sunshine, and we chose days when, after the sea breeze reaches the land, the wind direction was stable. We eventually chose 5 August 2016 as the case study date (Figure 10).

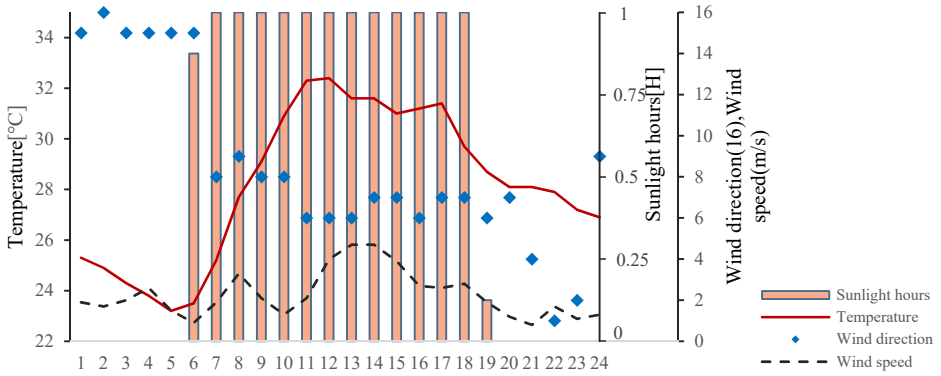

Figure 10. Meteorological characteristics of the case study day (5 August 2016). Includes sunlight hours, temperature, wind direction, and wind speed.

5. Mapping the Time of Summer Sea Breeze Event in Sendai City

5.1. Reproducibility Analysis of WRF Model Data

To verify the agreement of the WRF model with the measured data, we compared the WRF model simulation results with the long-term multi-point laboratory measurements (Table 3) where the simulated data were selected as the closest data point to the measurement point. Comparison of the results at each point showed a strong correlation between the simulated results and the long-term multi-point measurements, except for Higashishiromaru Primary School (point 19), where the correlation was 0.802. The correlations for the remaining measurement points were all greater than 0.9. The differences in RMSE were also small at each point, with four points being greater than 1 °C and the remaining points having RMSEs less than 1 °C. In total, 16 points of bias were around 1 °C. Analyzing the overall data in Higashi Nibancho Primary School (point 9) showed that the bias is 2.49 °C and the RMSE is 1 °C. It can be seen that the bias value of the model is larger in more urbanized areas. High bias values are also found in (point 11) (point 13) and (point 14), which are also distributed in more urbanized areas. The locations of points with high bias values are located near mountains and rivers, and the topography is more complex.

Table 3. Results of precision inspections for temperature numerical computation.

ID	Location	Bias (°C)	RMSE (°C)	Correlation
1	Nenoshiroishi	−0.55	0.68	0.981
2	Yakata	−0.88	0.82	0.973
3	Teraoka	−0.76	0.82	0.974
4	Nomura	−0.13	0.43	0.993
5	Kita-Sendai	−1.36	0.57	0.984
6	Kunimi	−1.81	0.53	0.985
7	Asahigaoka	−1.72	0.99	0.945
8	Tsurugaoka	−0.62	1.09	0.945
9	Higashi Nibancho	−2.49	1.00	0.936
10	Saiwaicho	−1.53	0.58	0.979
11	Nishitaga	−2.05	0.99	0.939
12	Hitokita	−0.24	0.88	0.969
13	Nagamachi	−2.13	0.86	0.950
14	Minamikoizumi	−2.15	0.88	0.937
15	Fukurobara	−0.84	1.03	0.912
16	Kabanomachi	−1.29	0.53	0.969
17	Takasago	−1.36	0.80	0.957
18	Rokugo	−1.20	0.82	0.926
19	Higashishiromaru	−0.60	1.34	0.802
20	Okada	−0.59	0.75	0.939

5.2. Sea Breeze Event Time Map and Discussion

5.2.1. Sea Breeze Arrival Time

We used the WRF simulation data to produce the sea breeze event time map and selected for the case study the date of 5 August 2016. Using the sea breeze arrival time defined in Section 4.1, the temperature data generated by the WRF at each point were read to identify the sea breeze arrival time at each point. Finally, a sea breeze arrival distribution map was generated using ArcGIS Pro (Figure 11a). The following is a detailed discussion of the sea breeze arrival time distribution chart.

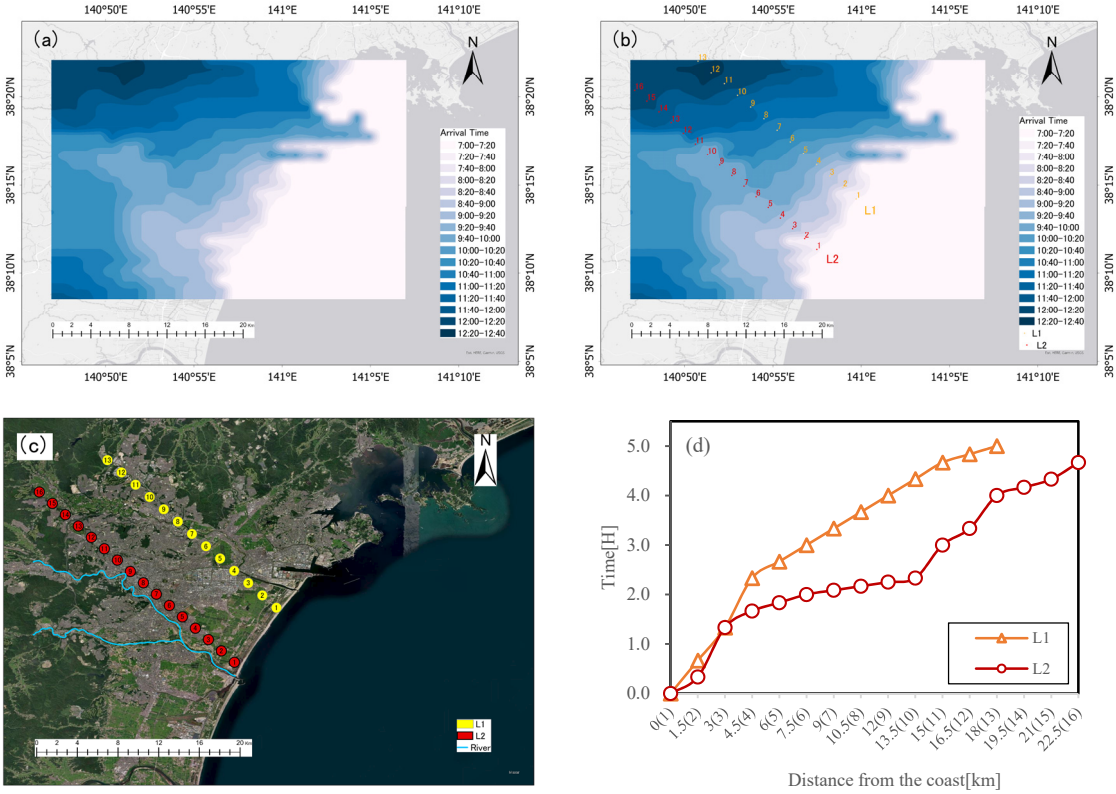

Figure 11. (**a**) Sea breeze arrival time map; (**b**) distribution of points in the L1 and L2 directions on the sea breeze arrival time map; (**c**) distribution of points in the L1 and L2 directions on the satellite map; (**d**) arrival times of points in the L1 and L2 directions.

At 7:00 to 12:40, sea breeze gradually penetrates inland from the coast (Figure 11a). In order to analyze the velocity, the points in two directions (L1 and L2) are arranged separately (Figure 11b). Figure 11c shows the location and environment of the points in the city. The points are consecutive, and both are spaced 1.5 km apart. The analysis of the sea breeze arrival time map and the line graph show that all parts close to the coast have a slower sea breeze blowing toward the land. In the line graph, L1 shows (Figure 11d) that the total time from point 1 (at 0 km) to point 4 (at 4.5 km) is 2 h and 20 min, and the speed is uniform. From point 4, the pace starts to pick up, reaching point 13 inland (at 18 km) in a total of 2 h and 40 min, a fast and even pace. L2 shows that the speed from point 1 (at km 0) to point 3 (at km 3) is about the same as L1. The speed increased rapidly from point 3, penetrating to point 10 (13.5 km) in one hour, after which the speed began to decrease. Overall, L1 is slower than L2. L2 reaches point 13 (at km 18) one hour ahead of L1.

As can be seen in Figure 11b, for the region from point 6 to point 10 in the L2 direction, the penetration of the sea breeze inland is significantly accelerated. In Figure 11c, it is found that points 6 to 10 are distributed near inland rivers. This is the same as the conclusion of Bastin's study that "inland rivers enhance the penetration of sea breeze inland" [26].

5.2.2. Sea Breeze Retreat Time

From 17:30 to 22:30, the sea breeze retreats toward the coast from inland areas, specifically from compact mid-rise and compact low-rise areas [50] (Figure 12a). We analyzed the sea breeze retreat time from three directions, with the retreat direction as the center point and according to the topography of Sendai (Figure 12b). Figure 12c shows the location and environment of the points in the city. According to Figure 12d, it can be seen that L1 is much faster than L2 and L3. The retreat from point 11 (at 15 km) to the coast took only 3 h and was fast and even. Additionally, L2 and L3 used a total of 4 h and 30 min to retreat from point 13 (at 18 km) to the coast. L2 began to decrease in speed at point 11 (at 15 km), increased in speed from point 9 (at 12 km) and retreated to the coast from point 5 (at 6 km) in 30 min. L3 retreated from point 13 (at 18 km) to point 8 (at 10.5 km) at about the same speed as L1, but after point 8, the speed decreased significantly. The decrease continued until point 4 (at 4.5 km), where the speed started to increase until it reached the coast. From Figure 12c, it can be found that the area where the retreat velocity of sea breeze decreases coincides with the urban edge, similar to Martilli's conclusion that "the roughness of the urban surface has a strong influence on the intensity of sea breeze" [30].

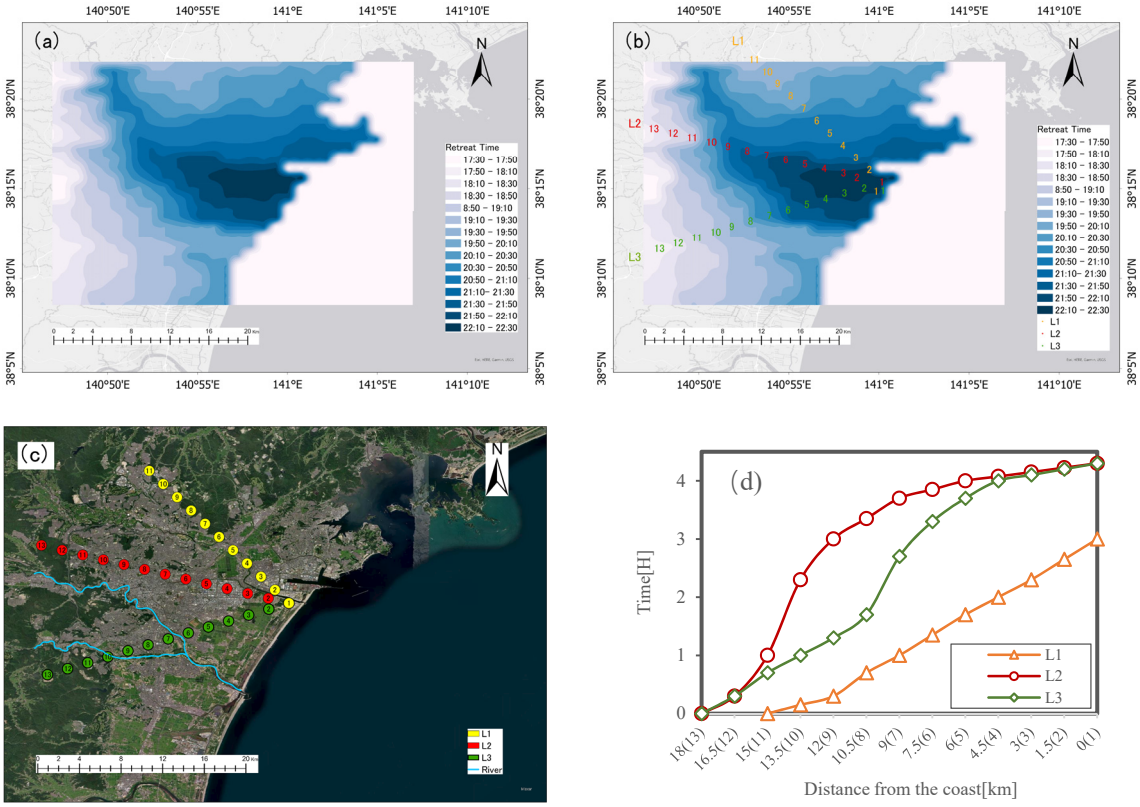

Figure 12. (**a**) Sea breeze retreat time map; (**b**) distribution of points in the L1, L2 and L3 directions on the sea breeze retreat time map; (**c**) distribution of points in the L1, L2 and L3 directions on the satellite map; (**d**) the time when the L1, L2, and L3 directions retreat to each point.

5.2.3. Duration of Sea Breeze

The sea breeze lasts for a minimum of 6 h and up to 15 h (Figure 13a). As can be seen from Figure 14, the duration increases gradually from inland to coastal times. The histogram in all three directions shows that the increase in duration is uniform and continuous (Figure 14a). Additionally, the total duration histogram showed that the cumulative duration of L1 and L3 was about the same. Additionally, in L2, the cumulative duration is about 13 h longer than in L1 and L3 (Figure 14b).

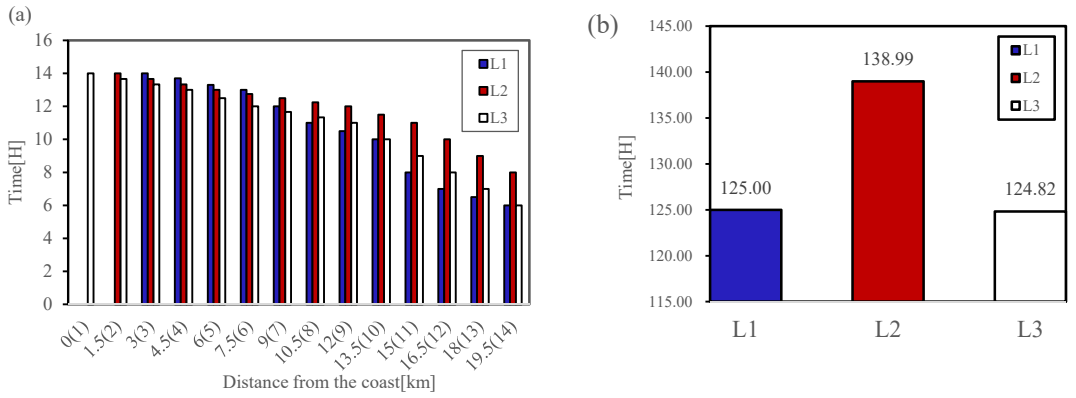

Figure 13. (**a**) The sea breeze duration at each point in the L1, L2 and L3 directions; (**b**) the sum of the sea breeze duration at all points in the L1, L2 and L3 directions.

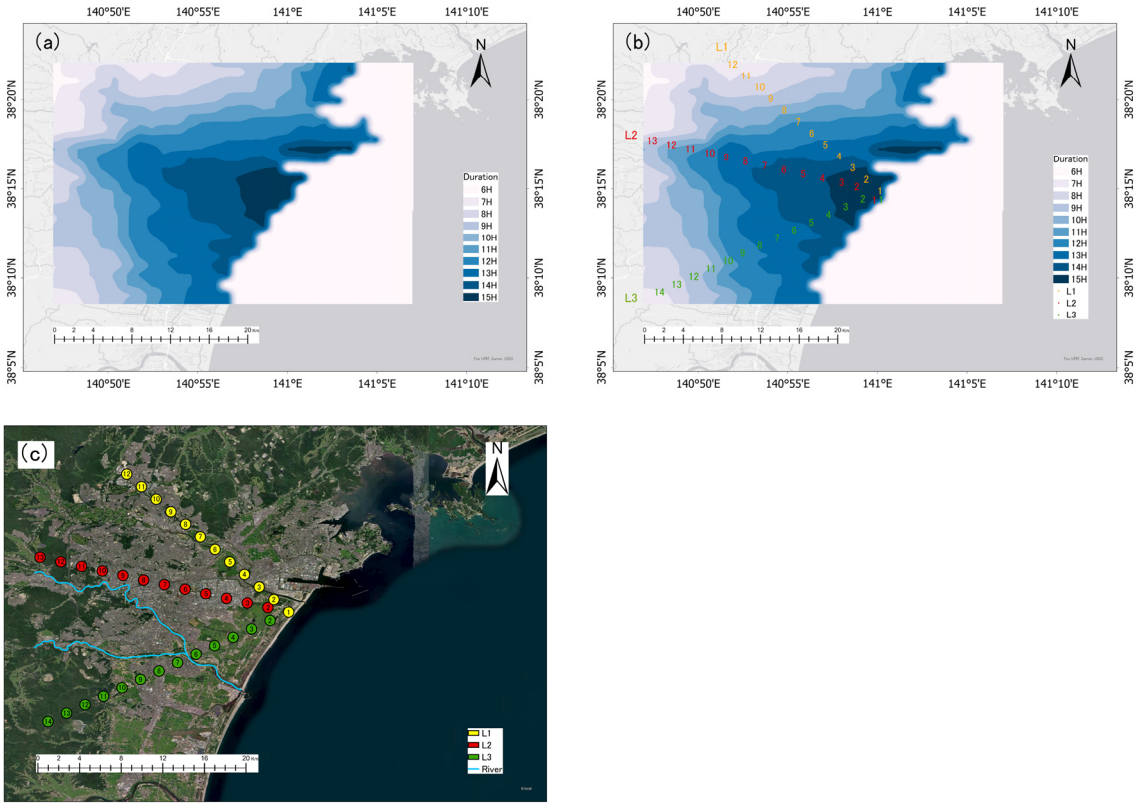

Figure 14. (**a**) Sea breeze duration time map; (**b**) distribution of points in the L1, L2 and L3 directions on the sea breeze duration time map; (**c**) distribution of points in the L1, L2 and L3 directions on the satellite map.

6. Conclusions

Sea breeze can effectively alleviate the summer heat in coastal cities. This study focuses on coastal cities and analyzes the temporal characteristics of the action of sea breeze in urban areas and the factors affecting its action. In the first stage, the long-term multi-point observation data were used to analyze their characteristics, and then, the calculation results of temperature and specific humidity from the WRF mesoscale meteorological model were used to produce a map of the temporal distribution of a sea breeze event. In the study, in the coastal part, the sea breeze blows landward at a slower rate, and the rate increases with penetration inland, as shown in the map of the sea breeze arrival time distribution. The arrival time of sea breeze is strongly influenced by inland rivers. From the map of sea breeze retreat time distribution, the direction of sea breeze retreat is related to the area of compact

mid-rise, compact low-rise and urban topography. The retreat of the sea breeze slows down significantly when it is close to highly urbanized areas. Until it is close to the coastal part, the sea breeze retreat speeds up. From the map of sea breeze duration distribution, the sea breeze duration is relatively evenly distributed in area, and the sea breeze duration is the longest in the direction of sea breeze retreat. In this study, the visualization of the sea breeze event time can visualize the distribution of the sea breeze event time, which has enriched the basic research on the relationship between sea breeze and cities.

Author Contributions: Conceptualization, S.P. and H.W.; methodology, S.P.; software, S.P.; validation, S.P. and H.W.; formal analysis, S.P.; investigation, S.P.; resources, S.P. and H.W.; data curation, S.P. and H.W.; writing—original draft preparation, S.P.; writing—review and editing, S.P. and H.W.; visualization, S.P.; supervision, H.W.; project administration, H.W.; funding acquisition, H.W. All authors have read and agreed to the published version of the manuscript.

Funding: This study was supported by the JSPS KAKENHI grant (no. JP19K04734), and the China Scholarship Council (no. 202008540002).

Acknowledgments: Thanks to the students in the lab for the discussion and study of technology.

Conflicts of Interest: The authors declare no conflict of interest. The funders had no role in the design of the study; in the collection, analyses, or interpretation of data; in the writing of the manuscript; or in the decision to publish the results.

References

1. Miller, S.T.K.; Keim, B.D.; Talbot, R.W.; Mao, H. Sea Breeze: Structure, Forecasting, and Impacts. *Rev. Geophys.* **2003**, *41*, 3. [CrossRef]
2. Hopkins, G.; Simmons, C.T. Temporal and Spatial Patterns of Air Temperature in a Coastal City with a Slope Base Setting. *J. Geophys. Res.-Atmos.* **2016**, *121*, 5336–5355. [CrossRef]
3. Kolokotsa, D.; Psomas, A.; Karapidakis, E. Urban Heat Island in Southern Europe: The Case Study of Hania, Crete. *Sol. Energy* **2009**, *83*, 1871–1883. [CrossRef]
4. Pokhrel, R.; Lee, H. Estimation of the Effective Zone of Sea/Land Breeze in a Coastal Area. *Atmos. Pollut. Res.* **2011**, *2*, 106–115. [CrossRef]
5. Dandou, A.; Tombrou, M.; Soulakellis, N. The Influence of the City of Athens on the Evolution of the Sea-Breeze Front. *Bound.-Layer Meteorol.* **2009**, *131*, 35–51. [CrossRef]
6. Shen, L.; Zhao, C.; Ma, Z.; Li, Z.; Li, J.; Wang, K. Observed Decrease of Summer Sea-Land Breeze in Shanghai from 1994 to 2014 and Its Association with Urbanization. *Atmos. Res.* **2019**, *227*, 198–209. [CrossRef]
7. Ma, Y.; Gao, R.Z.; Miao, S.G. Impacts of urbanization on summertime SLB circulation in Qingdao. *Acta Sci. Circumst.* **2013**, *33*, 1690–1696. [CrossRef]
8. Bei, N.; Zhao, L.; Wu, J.; Li, X.; Feng, T.; Li, G. Impacts of Sea-Land and Mountain-Valley Circulations on the Air Pollution in Beijing-Tianjin-Hebei (BTH): A Case Study. *Environ. Pollut.* **2018**, *234*, 429–438. [CrossRef]
9. Wang, S.; Zhu, J. Amplified or Exaggerated Changes in Perceived Temperature Extremes under Global Warming. *Clim. Dyn.* **2020**, *54*, 117–127. [CrossRef]
10. Brooke Anderson, G.; Bell, M.L. Heat Waves in the United States: Mortality Risk during Heat Waves and Effect Modification by Heat Wave Characteristics in 43 U.S. Communities. *Environ. Health Perspect.* **2011**, *119*, 210–218. [CrossRef]
11. Stewart, I.D.; Oke, T.R. Local Climate Zones for Urban Temperature Studies. *Bull. Am. Meteorol. Soc.* **2012**, *93*, 1879–1900. [CrossRef]
12. Golden, J.S.; Hartz, D.; Brazel, A.; Luber, G.; Phelan, P. A Biometeorology Study of Climate and Heat-Related Morbidity in Phoenix from 2001 to 2006. *Int. J. Biometeorol.* **2008**, *52*, 471–480. [CrossRef] [PubMed]
13. Guan, H.; Soebarto, V.; Bennett, J.; Clay, R.; Andrew, R.; Guo, Y.; Gharib, S.; Bellette, K. 14 Response of Office Building Electricity Consumption to Urban Weather in Adelaide, South Australia. *Urban Clim.* **2014**, *10*, 42–55. [CrossRef]
14. Park, H.S. Features of the Heat Island in Seoul and Its Surrounding Cities. *Atmos. Environ.* **1986**, *20*, 1859–1866. [CrossRef]
15. Kim, Y.H.; Baik, J.J. Daily Maximum Urban Heat Island Intensity in Large Cities of Korea. *Theor. Appl. Climatol.* **2004**, *79*, 151–164. [CrossRef]
16. He, B.J. Potentials of Meteorological Characteristics and Synoptic Conditions to Mitigate Urban Heat Island Effect. *Urban Clim.* **2018**, *24*, 26–33. [CrossRef]
17. Yow, D.M. Urban heat islands: Observations, impacts, and adaptation. *Geogr. Compass* **2007**, *1*, 1227–1251. [CrossRef]
18. Rajagopalan, P.; Lim, K.C.; Jamei, E. Urban Heat Island and Wind Flow Characteristics of a Tropical City. *Sol. Energy* **2014**, *107*, 159–170. [CrossRef]
19. Lopes, A.; Lopes, S.; Matzarakis, A.; Alcoforado, M.J. The Influence of the Summer Sea Breeze on Thermal Comfort in Funchal (Madeira). A Contribution to Tourism and Urban Planning. *Meteorol. Z.* **2011**, *20*, 553–564. [CrossRef]

20. Emmanuel, R.; Johansson, E. Influence of Urban Morphology and Sea Breeze on Hot Humid Microclimate: The Case of Colombo, Sri Lanka. *Clim. Res.* **2006**, *30*, 189–200. [CrossRef]
21. Masuda, Y.; Ikeda, N.; Seno, T.; Takahashi, N.; Ojima, T. A Basic Study on Utilization of the Cooling Effect of Sea Breeze in Waterfront Areas along Tokyo Bay. *J. Asian Archit. Build. Eng.* **2005**, *4*, 483–487. [CrossRef]
22. Archer, C.L.; Colle, B.A.; Delle Monache, L.; Dvorak, M.J.; Lundquist, J.; Bailey, B.H.; Beaucage, P.; Churchfield, M.J.; Fitch, A.C.; Kosovic, B.; et al. Meteorology for Coastal/Offshore Wind Energy in the United States: Recommendations and Research Needs for the next 10 Years. *Bull. Am. Meteorol. Soc.* **2014**, *95*, 515–519. [CrossRef]
23. Gilliam, R.C.; Raman, S.; Niyogi, D.E.V.D.S. Observational and Numerical Study on the Influence of Large-Scale flow Direction and Coastline Shape on Seabreeze Evolution. *Bound.-Layer Meteorol.* **2004**, *111*, 275–300. [CrossRef]
24. Takebayashi, H.; Tanaka, T.; Moriyama, M.; Watanabe, H.; Miyazaki, H.; Kittaka, K. Relationship between City Size, Coastal Land Use, and Summer Daytime Air Temperature Rise with Distance from Coast. *Climate* **2018**, *6*, 84. [CrossRef]
25. Freitas, E.D.; Rozoff, C.M.; Cotton, W.R.; Silva Dias, P.L. Interactions of an Urban Heat Island and Sea-Breeze Circulations during Winter over the Metropolitan Area of São Paulo, Brazil. *Bound.-Layer Meteorol.* **2007**, *122*, 43–65. [CrossRef]
26. Bastin, S.; Drobinski, P. Temperature and Wind Velocity Oscillations along a Gentle Slope during Sea-Breeze Events. *Bound.-Layer Meteorol.* **2005**, *114*, 573–594. [CrossRef]
27. Crosman, E.T.; Horel, J.D. Sea and Lake Breezes: A Review of Numerical Studies. *Bound.-Layer Meteorol.* **2010**, *137*, 1–29. [CrossRef]
28. Liu, R.; Han, Z.; Wu, J.; Hu, Y.; Li, J. The Impacts of Urban Surface Characteristics on Radiation Balance and Meteorological Variables in the Boundary Layer around Beijing in Summertime. *Atmos. Res.* **2017**, *197*, 167–176. [CrossRef]
29. Morini, E.; Touchaei, A.G.; Rossi, F.; Cotana, F.; Akbari, H. Evaluation of Albedo Enhancement to Mitigate Impacts of Urban Heat Island in Rome (Italy) Using WRF Meteorological Model. *Urban Clim.* **2018**, *24*, 551–566. [CrossRef]
30. Shen, L.; Sun, J.; Yuan, R. Idealized Large-Eddy Simulation Study of Interaction between Urban Heat Island and Sea Breeze Circulations. *Atmos. Res.* **2018**, *214*, 338–347. [CrossRef]
31. Varquez, A.C.G.; Nakayoshi, M.; Kanda, M. The Effects of Highly Detailed Urban Roughness Parameters on a Sea-Breeze Numerical Simulation. *Bound.-Layer Meteorol.* **2015**, *154*, 449–469. [CrossRef]
32. Martilli, A. A Two-Dimensional Numerical Study of the Impact of a City on Atmospheric Circulation and Pollutant Dispersion in a Coastal Environment. *Bound.-Layer Meteorol.* **2003**, *108*, 91–119. [CrossRef]
33. Peng, Z.; Hu, F. A study of the influence of urbanization of Beijing on the boundary wind structure. *Chin. J. Geophys.* **2006**, *49*, 1608–1615.
34. Hu, X.M. Influence of Synoptic Sea Breeze Fronts on the Urban Heat Island Intensity in Dallas-Fort Worth, Texas. *Syria Studies* **2015**, *7*, 37–72. [CrossRef]
35. David, E.K. Convection Initiation Associated with a Sea-Breeze Front, AGust Front, and Their Collision. *Mon. Weather. Rev.* **1995**, *123*, 2913–2933. [CrossRef]
36. Junimura, Y.; Watanabe, H. Study on the Effects of Sea Breeze for Decreasing Urban Air Temperature in Summer: Analyses Based on Long-Term Multi-Point Measurements and Observed Wind Conditions. *J. Environ. Eng. AIJ* **2008**, *73*, 93–99. [CrossRef]
37. Katayama, T.; Hayashi, T.; Shiotsuki, Y.; Kitayama, H.; Ishii, A.; Nishida, M.; Tsutsumi, J.I.; Oguro, M. Cooling Effects of a River and Sea Breeze on the Thermal Environment in a Built-up Area. *Energy Build.* **1991**, *16*, 973–978. [CrossRef]
38. Kitao, N.; Moriyama, M.; Takebayashi, H.; Tanaka, T. A Study on Making Method of a Study on Making Method of Climate Atlas in Osaka Region. *AIJ J. Technol. Des.* **2012**, *18*, 255–258. [CrossRef]
39. Peng, S.; Kon, Y.; Watanabe, H. Effects of Sea Breeze on Urban Areas Using Computation Fluid Dynamic—A Case Study of the Range of Cooling and Humidity Effects in Sendai, Japan. *Sustainability* **2022**, *14*, 1074. [CrossRef]
40. Khan, S.M.; Simpson, R.W. Effect of a Heat Island on the Meteorology of a Complex Urban Airshed. *Bound.-Layer Meteorol.* **2001**, *100*, 487–506. [CrossRef]
41. Naor, R.; Potchter, O.; Shafir, H.; Alpert, P. An Observational Study of the Summer Mediterranean Sea Breeze Front Penetration into the Complex Topography of the Jordan Rift Valley. *Theor. Appl. Climatol.* **2017**, *127*, 275–284. [CrossRef]
42. Powers, J.G.; Klemp, J.B.; Skamarock, W.C.; Davis, C.A.; Dudhia, J.; Gill, D.O.; Coen, J.L.; Gochis, D.J.; Ahmadov, R.; Peckham, S.E.; et al. The Weather Research and Forecasting Model: Overview, System Efforts, and Future Directions. *Bull. Am. Meteorol. Soc.* **2017**, *98*, 1717–1737. [CrossRef]
43. Skamarock, W.C.; Klemp, J.B.; Dudhia, J.; Gill, D.O.; Barker, D.M. A Description of the Advanced Research WRF Version 3. NCAR Tech. Note NCAR/TN-475+STR. 2008. 113p. Available online: https://opensky.ucar.edu/islandora/object/technotes:500 (accessed on 25 July 2022).
44. Miao, Y.; Liu, S.; Chen, B.; Zhang, B.; Wang, S.; Li, S. Simulating Urban Flow and Dispersion in Beijing by Coupling a CFD Model with the WRF Model. *Adv. Atmos. Sci.* **2013**, *30*, 1663–1678. [CrossRef]
45. Zheng, Y.; Miao, Y.; Liu, S.; Chen, B.; Zheng, H.; Wang, S. Simulating Flow and Dispersion by Using WRF-CFD Coupled Model in a Built-up Area of Shenyang, China. *Adv. Meteorol.* **2015**, *2015*, 528618. [CrossRef]
46. Kusaka, H.; Hara, M.; Takane, Y. Urban Climate Projection by the WRF Model at 3-Km Horizontal Grid Increment: Dynamical Downscaling and Predicting Heat Stress in the 2070's August for Tokyo, Osaka, and Nagoya Metropolises. *J. Meteorol. Soc. Jpn.* **2012**, *90*, 47–63. [CrossRef]

47. Hong, S.Y.; Dudhia, J.; Chen, S.H. A Revised Approach to Ice Microphysical Processes for the Bulk Parameterization of Clouds and Precipitation. *Mon. Weather. Rev.* **2004**, *132*, 103–120. [CrossRef]
48. Xie, B.; Fung, J.C.H.; Chan, A.; Lau, A. Evaluation of Nonlocal and Local Planetary Boundary Layer Schemes in the WRF Model. *J. Geophys. Res. Atmos.* **2012**, *117*, 1–26. [CrossRef]
49. Kain, J.S. The Kain–Fritsch Convective Parameterization: An Update. *J. Appl. Meteorol.* **2004**, *43*, 170–181. [CrossRef]
50. Zhou, X.; Okaze, T.; Ren, C.; Cai, M.; Ishida, Y.; Watanabe, H.; Mochida, A. Evaluation of Urban Heat Islands Using Local Climate Zones and the Influence of Sea-Land Breeze. *Sustain. Cities Soc.* **2020**, *55*, 102060. [CrossRef]